Critical currents and supercurrent oscillations in Josephson field-effect transistors

A. Chrestin, T. Matsuyama, and U. Merkt
Institut für Angewandte Physik, Universität Hamburg, Jungiusstrasse 11, D-20355 Hamburg, Federal Republic of Germany
(Received 29 June 1993)

The dc Josephson effect of a superconductor/two-dimensional electron gas/superconductor (S/2DEG/S) junction in the clean limit is investigated with emphasis on the field-effect dependence of the critical current. Calculation of the Josephson current is based on solving the Bogoliubov–de Gennes equations for a steplike variation of the pair potential. In the normal conducting region, the motion of electrons is quantized in one direction by means of a triangular-well potential. The 2DEG is contained in a semiconductor treated within the effective-mass approximation. We assume an abrupt band-edge jump at the interfaces, and additional scattering is taken into account by δ-function potential barriers. Normal scattering leads to the formation of resonant states, which are visible in critical current oscillations. The ratio of Fermi velocities in the 2DEG and the S regions determines the rates of Andreev and normal scattering and has a large influence on the field-effect dependence of the critical current. We take an effective mass suitable for the inversion layer on p-type InAs and consider Nb for the superconducting contacts. Typical magnitudes of the calculated critical current are some μA-per-μm junction width for experimentally accessible values of junction length, temperature, and surface carrier density of the 2DEG.

I. INTRODUCTION

Superconducting three-terminal devices have attracted great interest for several years.[1] They can be realized as weak links coupled by a two-dimensional electron gas (2DEG), in which the Josephson current is controlled via a gate voltage (Josephson field-effect transistor). Low carrier effective mass, high mobility, and the absence of Schottky barriers at the superconductor/semiconductor (S/Sm) interfaces are favorable properties of InAs as a material for the semiconductor. Supercurrents in 2D electron systems based on InAs have been reported by several authors.[2–5] Theoretical investigations of supercurrents in a Josephson field-effect transistor have been published by Kresin for the limit of long junctions[6] and, for $T \approx T_c$, by Tanaka and Tsukada,[7,8] who considered a one-dimensional model.

This paper is mainly concerned with the question of how the Josephson current is influenced by the abrupt change of electron effective mass, the band-edge jump, and the change from a 3D electron system to a 2DEG at the S/Sm interfaces. We restrict ourselves to ballistic transport ($l \gg L$) in the clean limit ($l \gg \xi_N$), where l, L, and ξ_N denote the mean free path, the junction length, and the coherence length in the Sm region, respectively. In the clean limit, the latter is given by $\xi_N = \hbar v_F/(2\pi k_B T)$, where v_F is the Fermi velocity of the Sm region.[9] The geometry of our model is based on the device geometry used by Takayanagi and Kawakami.[4] The 2DEG in their device, which has been operating in the dirty limit ($l \ll \xi_N$), is an inversion layer on the surface of p-type InAs. Two-dimensional electron systems in the clean limit may be realized in semiconductor heterostructures.[2,3] To calculate the Josephson current, we employ a method proposed by Furusaki *et al.*[10,11] Our result is valid for any junction length and all temperatures, except for the immediate vicinity of T_c.

II. BASIC ASSUMPTIONS

The device geometry assumed for our calculation is shown in Fig. 1. The system is described by the Bogoliubov–de Gennes equations,[12]

$$\begin{pmatrix} \mathcal{H} & \Delta(\mathbf{r}) \\ \Delta^*(\mathbf{r}) & -\mathcal{H} \end{pmatrix} \begin{pmatrix} u(\mathbf{r}) \\ v(\mathbf{r}) \end{pmatrix} = E \begin{pmatrix} u(\mathbf{r}) \\ v(\mathbf{r}) \end{pmatrix} . \quad (1)$$

Solutions to this equation are electronlike and holelike quasiparticle (QP) wave functions.[13] The operator $\mathcal{H}$ is defined as

$$\mathcal{H} = -\frac{\hbar^2}{2}\nabla\frac{1}{m^*(x)}\nabla + U(\mathbf{r}) - \mu . \quad (2)$$

We take the effective-mass approximation (EMA) for the semiconductor, i.e., $m^*(x)$ is equal to some constant value m^* in the Sm region ($0 < x < L$) and equal to the free electron mass m_e in the superconductors $S1$ ($x < 0$) and $S2$ ($x > L$). At the conduction band edge of InAs,

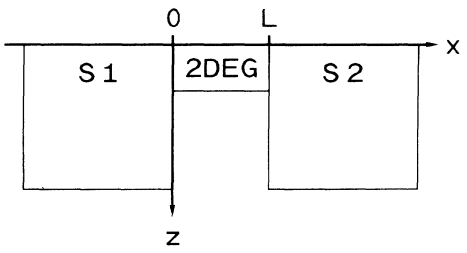

FIG. 1. Device geometry of an S/2DEG/S system.

the effective mass is $m_0^* = 0.023 m_e$. The chemical potential is given by $\mu = 5.32$ eV for Nb, $\Delta(\mathbf{r})$ is the superconducting pair potential. The potential $U(\mathbf{r})$ is written as $U(\mathbf{r}) = U_1(x) + U_2(y) + U_3(z)$. Translational invariance with periodic boundary conditions in the y direction is assumed, hence $U_2(y) = 0$ throughout the system.

The Nb contacts are modeled as half-infinite slabs of thickness W, occupying the regions $S1$ and $S2$, respectively. Therefore, for $x < 0$ and $x > L$,

$$U_3(z) = \begin{cases} 0\,, & 0 < z < W, \\ \infty\,, & z < 0,\ z > W\,. \end{cases} \tag{3}$$

A typical value for the Nb film thickness is $W \approx 100$ nm.[4] For $0 < x < L$, the confining potential is described by a triangular well,

$$U_3(z) = \begin{cases} \infty, & z < 0, \\ eF_s z, & z > 0\,. \end{cases} \tag{4}$$

This approximates the potential of an inversion layer,[14] the surface electrical field being given by F_s. In the x direction, we model the variation of the potential as

$$U_1(x) = U_0\,[\Theta(x) - \Theta(x-L)] + \frac{\hbar^2 p_F}{m_e}\,Z\,[\delta(x) + \delta(x-L)]\,. \tag{5}$$

Here we account for the different distances between the chemical potential and conduction band edge in the S and Sm regions, respectively, in the simplest possible way by introducing a potential step of height U_0. Additional scattering at the interfaces due to deviations from this idealization is taken into account by potential barriers of dimensionless strength Z.[13] The quantity $p_F = \sqrt{2m_e\mu/\hbar^2}$ denotes the Fermi wave number of the superconductors.

In principle, the superconducting pair potential has to be obtained self-consistently.[12] For simplicity, we assume a steplike change of the pair potential at the S/SM interfaces,

$$\Delta(\mathbf{r}) = \Delta(x) = \begin{cases} \Delta_0, & x < 0, \\ 0, & 0 < x < L, \\ \Delta_0 e^{i\varphi}, & x > L\,, \end{cases} \tag{6}$$

where $\Delta_0 = \Delta_0(T)$ is the modulus of the pair potential [$\Delta_0(0) = 1.5$ meV and $T_c = 9.2$ K for Nb], and φ is the phase difference of the pair potential across the junction. This ansatz is frequently used in the literature. According to the theory of Tanaka and Tsukada,[15] we expect only a weak deformation of the pair potential caused by the proximity effect. The reason is that only states of low momenta in the y and z directions in the superconductors can contribute to a leakage of Cooper pairs into the 2DEG.[16] Only when $T \to T_c$, the density of pairs in the superconductors becomes so small that any additional loss has to be taken into account. In this limit, the validity of the ansatz in Eq. (6) fails. Our model of the $S/2\mathrm{DEG}/S$ system is similar in many respects to the model of Schüssler and Kümmel,[17] who considered an $S/Sm/S$ contact with the 3D electron system of n-type InAs in the Sm region.

III. CALCULATION OF THE CURRENT

The system introduced above is compatible with the assumptions of Refs. 10 and 11. In these publications, four independent wave functions are considered for each QP energy, namely those of e-like and h-like QP's, incoming from $x = \pm\infty$. It turns out that the wave functions describing the e-like QP's incoming from $x = -\infty$ are sufficient to obtain the Josephson current. In our model, they are given by

$$\Psi_{1,j}(x,z;k_y) = \begin{cases} e^{ip_j^+ x}\varphi_j(z)\begin{pmatrix} u_0 \\ v_0 \end{pmatrix} + \sum_k \left[a_{1jk} e^{ip_k^- x}\begin{pmatrix} v_0 \\ u_0 \end{pmatrix} + b_{1jk} e^{-ip_k^+ x}\begin{pmatrix} u_0 \\ v_0 \end{pmatrix}\right]\varphi_k(z), & x < 0, \\ \sum_m \left[\left(\alpha_{1jm} e^{ik_m^+ x} + \beta_{1jm} e^{-ik_m^+(x-L)} \right)\begin{pmatrix} 1 \\ 0 \end{pmatrix} \right. \\ \left. + \left(\gamma_{1jm} e^{ik_m^-(x-L)} + \delta_{1jm} e^{-ik_m^- x} \right)\begin{pmatrix} 0 \\ 1 \end{pmatrix}\right]\zeta_m(z), & 0 < x < L, \\ \sum_k \left[c_{1jk} e^{ip_k^+(x-L)}\begin{pmatrix} u_0 e^{i\varphi/2} \\ v_0 e^{-i\varphi/2} \end{pmatrix} + d_{1jk} e^{-ip_k^-(x-L)}\begin{pmatrix} v_0 e^{i\varphi/2} \\ u_0 e^{-i\varphi/2} \end{pmatrix}\right]\varphi_k(z), & x > L\,. \end{cases} \tag{7}$$

Due to translational invariance, the motion in the y direction is completely determined by the wave number k_y of the corresponding plane wave. The index 1 at $\Psi_{1,j}$ is a reminder that there are other types of wave functions as noted above, the index j labels the state of motion in the z direction of the incoming QP. Motion in this direction in the S and Sm regions is described by the wave functions

$$\varphi_j(z) = \sqrt{\frac{2}{W}}\,\sin(q_j z) \tag{8}$$

with $q_j = (\pi/W)\,j$ and

$$\zeta_m(z) = \frac{1}{\sqrt{\mathcal{N}_m}}\,\mathrm{Ai}\left(\frac{z}{D} - \frac{E_m}{eF_s D}\right)\,, \tag{9}$$

respectively. The energies E_m are the subband edges in the inversion layer, the length $D = [\hbar^2/(2m^* eF_s)]^{1/3}$ is the characteristic spread of the subband wave functions $\zeta_m(z)$.[14] The normalization constant $\mathcal{N}_m = D[\mathrm{Ai}'(a_m)]^2$ is obtained by evaluating integrals of Airy functions,[18] a_m are the zeroes of the Airy function Ai.[19] Some further

definitions are introduced as follows:

$$p_j^{\pm} = \sqrt{p_F^2 - k_y^2 - q_j^2 \pm \frac{2m_e}{\hbar^2}\Omega}\,, \tag{10a}$$

$$\Omega = \sqrt{E^2 - \Delta_0^2}\,, \tag{10b}$$

$$k_m^{\pm} = \sqrt{k_{F,m}^2 - k_y^2 \pm \frac{2m^*}{\hbar^2}E}\,, \tag{10c}$$

$$k_{F,m} = \sqrt{\frac{2m^*}{\hbar^2}(\mu - U_0 - E_m)}\,, \tag{10d}$$

$$u_0 = \sqrt{\frac{1}{2}\left(1 + \frac{\Omega}{E}\right)}\,, \quad v_0 = \sqrt{\frac{1}{2}\left(1 - \frac{\Omega}{E}\right)}\,. \tag{10e}$$

The coefficients a_{1jk} and b_{1jk} are the amplitudes of reflection of the incoming e-like QP as an h-like QP and as an q-like QP, respectively. Equally, transmission into $S2$ is determined by c_{1jk} and d_{1jk}. The indices indicate that motion in the z direction is being changed from state j to k in these processes. Transmission between the superconductors can proceed via all possible electron and hole states in any subband m in the 2DEG, with amplitudes α_{1jm} to δ_{1jm}.

The method explained in Refs. 10 and 11 leads to the following expression for the Josephson current per unit junction width:

$$\langle i \rangle = \frac{e\Delta_0}{2\hbar} k_B T \sum_{\omega_n} \frac{1}{\Omega_n} \times \frac{1}{2\pi}\int_{-\infty}^{\infty} dk_y \sum_j \frac{p_j^+ + p_j^-}{p_j^+}\left[a_{1jj}(\varphi) - a_{1jj}(-\varphi)\right]. \tag{11}$$

All energy dependencies have to be replaced by Matsubara frequencies $\omega_n = (2n+1)\pi k_B T$ by means of analytic continuation, $E + i\delta \to i\omega_n$, and $\Omega_n = \sqrt{\omega_n^2 + \Delta_0^2}$. The coefficients a_{1jj} are obtained by solving the linear system of equations that arises from the boundary conditions to the wave function at $x = 0$ and $x = L$ (see the Appendix). An analytical solution of this system of equations can be found when scattering of QP's between different subbands at the S/Sm interfaces is neglected. It is shown in the Appendix that this only leads to minor errors. Because only QP's near the Fermi energy contribute to the current, i.e., $|\Omega| \ll \mu$, we disregard the dependence of $p_j^{\pm}$ on Ω in our calculation. The resulting current contribution of the subband m is

$$\langle i \rangle_m = -\frac{ek_BT}{\hbar}\sum_{\omega_n}\frac{1}{2\pi}\int_{-\infty}^{\infty}\frac{\sin\varphi}{\frac{1}{2}\cos\varphi + f_m(k_y,\omega_n)}\,dk_y\,, \tag{12}$$

$$f_m(k_y,\omega_n) = \eta_1^- e^{i(k_m^+ - k_m^-)L} + \eta_1^+ e^{-i(k_m^+ - k_m^-)L} - \eta_2^- e^{i(k_m^+ + k_m^-)L} - \eta_2^+ e^{-i(k_m^+ + k_m^-)L}\,, \tag{13}$$

$$\eta_1^{\pm} = \frac{1}{16}\frac{\sigma^2 p^2}{k_m^+ k_m^-}\left\{\frac{\Omega_n}{\Delta_0}\left[1 + \left(2Z\frac{p_F}{p}\right)^2 + \frac{k_m^+ k_m^-}{\sigma^2 p^2}\right] \pm \left(\frac{\omega_n}{\Delta_0}\frac{k_m^+ + k_m^-}{\sigma p} - 2iZ\frac{p_F}{p}\frac{\Omega_n}{\Delta_0}\frac{k_m^+ - k_m^-}{\sigma p}\right)\right\}^2, \tag{14}$$

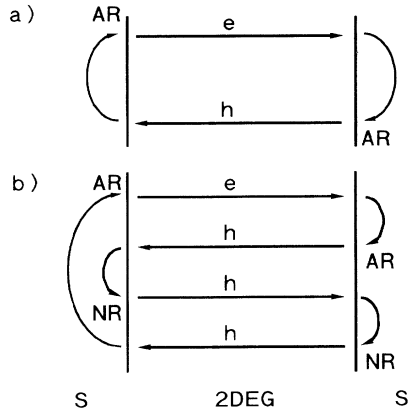

FIG. 2. (a) Multiple Andreev reflection (AR) process. An electron (e) is retroreflected as a hole (h) and vice versa at the S/Sm interfaces. (b) One process contributing to the oscillatory terms in Eq. (13). The lowest-order term contributing to the oscillations involves two Andreev (AR) and two normal (NR) reflections.

$$\eta_2^{\pm} = \frac{1}{16}\frac{\sigma^2 p^2}{k_m^+ k_m^-}\left\{\frac{\Omega_n}{\Delta_0}\left[1 + \left(2Z\frac{p_F}{p}\right)^2 - \frac{k_m^+ k_m^-}{\sigma^2 p^2}\right] \pm \left(\frac{\omega_n}{\Delta_0}\frac{k_m^+ - k_m^-}{\sigma p} - 2iZ\frac{p_F}{p}\frac{\Omega_n}{\Delta_0}\frac{k_m^+ + k_m^-}{\sigma p}\right)\right\}^2. \tag{15}$$

We use the abbreviations $\sigma = m^*/m_e$ and $p = \sqrt{p_F^2 - k_y^2}$. In general, the integrand is non-negligible in the whole range $|k_y| < k_{F,m}$, but very small otherwise. Equation (12) for the Josephson current is equivalent to the one derived by Furusaki *et al.* for a superconducting quantum point contact with finite barrier strength, when we put $k_m^+ = k_m^- = p$ and $\sigma = 1$ in $\eta_{1,2}^{\pm}$.[11]

The first two terms in Eq. (13) are due to a multiple Andreev reflection of QP's running back and forth inside the 2DEG, as shown in Fig. 2(a). The remaining two terms arise when normal reflection is taken into account, which must not be neglected in S/Sm systems, even for $Z = 0$. One process contributing to these terms is sketched in Fig. 2(b). They are caused by the interference of QP's that undergo Andreev as well as normal reflection. This interference leads to critical current oscillations, as will be seen in the following section. Similar oscillations have been analyzed by Gudkov *et al.*,[20] who observed them in the 3D electron system of α-Si. They were also discussed in connection with a superconducting quantum point contact in Ref. 11.

IV. DISCUSSION

The functional behavior of the current contributions of various subbands is identical, only the magnitude of $k_{F,m}$ is different. To keep the subsequent discussion transparent, a single occupied subband is assumed. The subband indices will therefore be omitted in this section. In the one-subband case, the Fermi wave number in the 2DEG is related to the surface carrier density n_s by $k_F = \sqrt{2\pi n_s}$.

Thus n_s fixes the value of $U_0 + E_0$, see Eq. (10d). First we consider ideal S/Sm contacts with barrier strength $Z = 0$. The influence of a finite barrier strength is discussed at the end of this section.

The critical current dependence on carrier density is shown in Fig. 3. The position of the maxima, as well as the large variation in amplitude of the oscillations, can be understood by looking at the dominant contribution to the last two terms in Eq. (13). For $Z = 0$, this is given by

$$-\frac{1}{2}\left[\frac{\Omega_n}{2\Delta_0}\left(\frac{\sigma p}{\sqrt{k^+k^-}}-\frac{\sqrt{k^+k^-}}{\sigma p}\right)\right]^2\cos\left[(k^+ + k^-)L\right]$$

$$\approx -\frac{1}{2}\left[\frac{\Omega_n}{2\Delta_0}\left(\frac{\tilde{v}(k_y)}{v(k_y)}-\frac{v(k_y)}{\tilde{v}(k_y)}\right)\right]^2\cos\left(2\sqrt{k_F^2-k_y^2}L\right)\,. \tag{16}$$

Here we introduced the velocities $v(k_y) := \hbar/m^*\sqrt{k_F^2-k_y^2}$ and $\tilde{v}(k_y) = \hbar/m_e\sqrt{p_F^2-k_y^2}$ for the Sm region and for the S regions, respectively. Equal velocities mean that no normal reflection occurs for the corresponding QP states. The oscillations are strongly suppressed when the Fermi velocities $v_F \equiv v(0)$ and $\tilde{v}(0)$ are nearly equal, because then normal reflection is suppressed for QP's with large velocities in the direction of the current flow, which contribute most to the current. For $m^* = m_0^*$, this is the case at $n_s \approx 1.2\times10^{12}$ cm^{-2}. Local maxima of the critical current as a function of carrier density are well approximated by the relation

$$n_{s,\max} = \frac{\pi}{2L^2}N^2\,. \tag{17}$$

The integer N equals half the number of QP states with "resonant" values of k_y, defined by maxima of the cosine in Eq. (16).

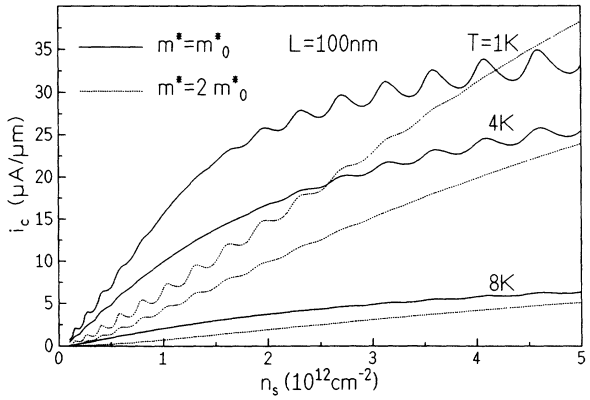

FIG. 3. Surface carrier density dependence of the critical current for $Z = 0$. The current is evaluated for the band-edge effective mass of InAs, $m_0^* = 0.023m_e$, and for $2m_0^*$ at various temperatures. Two different values of effective mass are considered in order to mimic band nonparabolicity.

The average behavior of the current as a function of n_s is determined by the multiple Andreev reflection terms. An exponential increase $\sim e^{-L/\xi_N}$ [see Eq. (19), $\xi_N(n_s) = \hbar^2\sqrt{2\pi n_s}/(2\pi m^* k_B T)$] is found at low carrier densities, when $\xi_N(n_s) \lesssim L$. For $L = 100$ nm (Fig. 3) and $m^* = m_0^*$, this is the case only up to densities $n_s \approx 2.7\times10^{11}$ cm^{-2} at $T = 8$ K, and even smaller densities for lower temperatures. In this region, increasing overlap of the Cooper pair density in the Sm region is responsible for the exponential growth of the current. At larger carrier densities, instead of the coherence length, Andreev reflection probability plays a major role, which is contained in the amplitudes $\eta_1^{\pm}$ of the multiple Andreev reflection terms. Their n_s dependence is mainly contained in the term

$$\left(\frac{\sigma p}{\sqrt{k^+k^-}}+\frac{\sqrt{k^+k^-}}{\sigma p}\right)\approx\left(\frac{\tilde{v}(k_y)}{v(k_y)}+\frac{v(k_y)}{\tilde{v}(k_y)}\right)\,. \tag{18}$$

This term goes through a minimum at $v(k_y) = \tilde{v}(k_y)$, where Andreev reflection is most probable and normal reflection disappears. As noted above, for $m^* = m_0^*$ the Fermi velocities coincide at $n_s = 1.2\times10^{12}$ cm^{-2}. The current saturates when n_s becomes much larger, because in this case $v(k_y) \gg \tilde{v}(k_y)$ for most contributing states, which is unfavorable for Andreev reflection. A residual increase is attributed to the growing number of current carrying states. In our model, we find that the current in this region increases more slowly than $\propto \sqrt{n_s}$, the behavior obtained in Ref. 6.

In Fig. 4, a semilogarithmic plot of the length dependence of the critical current is shown. For $L \gg \xi_N$, the following approximation can be derived, taking into account only the lowest Matsubara frequency:[16]

$$\langle i\rangle \approx -\frac{32}{\sqrt{2\pi^5}}\,\frac{e\Delta_0^2}{\hbar k_B T}\,k_F\frac{1}{a^2\sqrt{\frac{L}{\xi_N}+b}}\,e^{-L/\xi_N}\,\sin\varphi \tag{19}$$

with the abbreviations

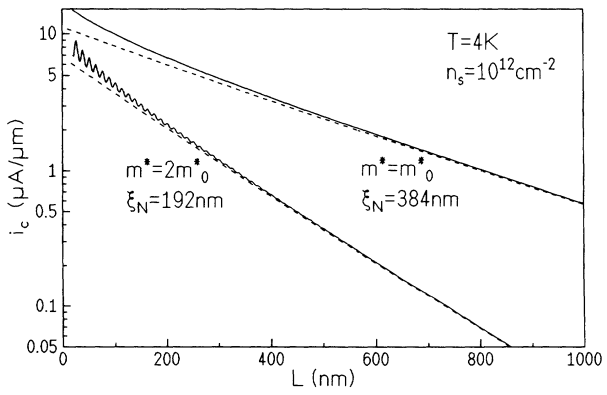

FIG. 4. Length dependence of the critical current for $Z = 0$. The dashed curves represent the long junction approximation according to Eq. (19).

$$a = 2 + \sqrt{1 + \left(\frac{\Delta_0}{\pi k_B T}\right)^2}\left(\frac{\tilde{v}(0)}{v(0)} + \frac{v(0)}{\tilde{v}(0)}\right) , \qquad (20a)$$

$$b = \frac{1}{4} + \frac{4}{a}\left[1 + \sqrt{1 + \left(\frac{\Delta_0}{\pi k_B T}\right)^2}\frac{\tilde{v}(0)}{v(0)}\right] . \qquad (20b)$$

This relation contains the usual asymptotically exponential decay of the current. The coherence length ξ_N is no longer a useful length scale for the current when $L < \xi_N$, since higher Matsubara frequencies become important. For $T \to 0$, the approximation of Eq. (19) is valid only in the limit $L \to \infty$ because the coherence length ξ_N diverges. This explains why in this approximation $\langle i \rangle$ disappears for $T \to 0$. The approximation of Eq. (19) is represented by the dashed curves in Fig. 4. The amplitude of the oscillations decays asymptotically as e^{-2L/ξ_N}, because at least four crossings of the Sm region are necessary [Fig. 2(b)], whereas the lowest-order multiple Andreev reflection process requires only two crossings [Fig. 2(a)]. Equation (17) yields the position of local maxima, $L_{\max} = (\lambda_F/2)\,N$, with $\lambda_F = 2\pi/k_F$.

The temperature dependence depicted in Fig. 5 shows that the current remains low unless the temperature is well below T_c when $L \gg \xi_N(T_c)$. For the carrier density $n_s = 10^{12}$ cm^{-2} of Fig. 5, $\xi_N(T_c) = 167$ and 83 nm for m_0^* and $2m_0^*$, respectively. It may therefore be necessary to go to rather low temperatures to have a measurable critical current. As long as one can neglect suppression of the pair potential, the current behaves as $(1 - T/T_c)$ near T_c. A crossover from $(1-T/T_c)^2$ behavior[21] to $(1 - T/T_c)$ behavior was predicted by Tanaka and Tsukada[7] for systems with a weak proximity effect.

Finally, we look at the influence of a finite barrier strength on the current. Figure 6 shows the n_s dependence for different values of Z. Additional scattering by the barrier reduces Andreev reflection and increases normal reflection. As a result, the mean current is lowered, whereas the oscillations become more pronounced with increasing Z. Even when both Fermi velocities coincide, normal reflection due to a finite Z parameter leads to visible oscillations. Since the barrier strength influences the matching conditions at the interfaces, the resonant QP

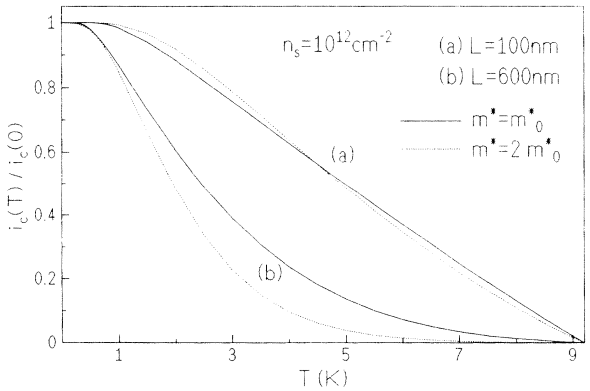

FIG. 5. Temperature dependence of the critical current for $Z = 0$. The absolute current values at $T = 0$ are 15.8 μA/μm (L = 100 nm, $m^* = m_0^*$), 6.9 μA/μm (100 nm, $2m_0^*$), 7.9 μA/μm (600 nm, m_0^*), and 2.2 μA/μm (600 nm, $2m_0^*$).

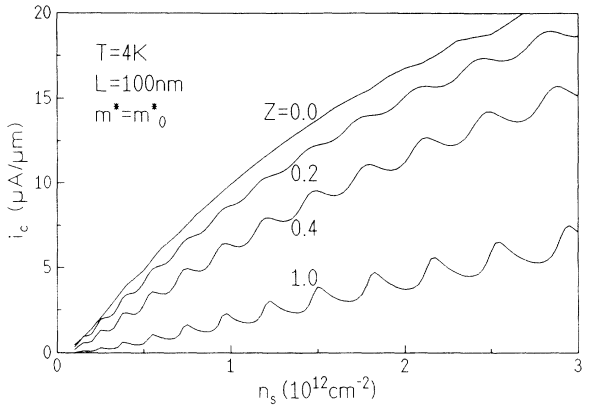

FIG. 6. Influence of a finite barrier potential on the critical current. Normal reflection increases, Andreev reflection decreases with growing barrier strength Z. Therefore the mean current is reduced and the oscillations become more pronounced with increasing Z.

states and therefore the positions of the maxima shift depending on Z.

V. CONCLUSION

Josephson currents in clean S/2DEG/S systems have been investigated. For junction lengths accessible to modern preparation techniques, it has been demonstrated that Andreev and normal reflection probabilities are important parameters for the field-effect dependence of the current. In accordance with the results of Kresin,[6] the strongest field-effect dependence is found for low carrier densities. We have investigated amplitude and period of oscillations of the critical current caused by the presence of normal reflection. In 2D systems, experimental verification of these resonance effects will be most easily performed by varying the carrier density via the field effect. This parameter can be more exactly controlled than the junction length. Short junctions and low temperatures favor large amplitudes because of the exponential decay on a length scale $\xi_N/2$. The spacing $\lambda_F/2$ of the maxima poses rather stringent conditions on the smoothness of the S/Sm contacts in order to observe the oscillations. The same effects investigated here for an inversion layer should also be present in other 2D electron systems, e.g., in semiconductor heterostructures. Success in the preparation of these S/2DEG/S systems has been reported.[2,3] Because of the high electron mobility in these devices, we expect that the results of our calculation can be tested in the near future.

ACKNOWLEDGMENTS

We thank Kurt Scharnberg for valuable discussions and the Deutsche Forschungsgemeinschaft for financial support.

APPENDIX

The adequate boundary conditions for our wave function and its derivative are[22]

$$\Psi(\mathbf{r})|_{x=0^-} = \Psi(\mathbf{r})|_{x=0^+} , \tag{A1a}$$

$$\Psi(\mathbf{r})|_{x=L^-} = \Psi(\mathbf{r})|_{x=L^+} , \tag{A1b}$$

$$\frac{\hbar^2}{2m^*}\frac{\partial}{\partial x}\Psi(\mathbf{r})|_{x=0^+} - \frac{\hbar^2}{2m_e}\frac{\partial}{\partial x}\Psi(\mathbf{r})|_{x=0^-} = \frac{\hbar^2 p_F}{m_e} Z\,\Psi(\mathbf{r})|_{x=0} , \tag{A1c}$$

$$\frac{\hbar^2}{2m_e}\frac{\partial}{\partial x}\Psi(\mathbf{r})|_{x=L^+} - \frac{\hbar^2}{2m^*}\frac{\partial}{\partial x}\Psi(\mathbf{r})|_{x=L^-} = \frac{\hbar^2 p_F}{m_e} Z\,\Psi(\mathbf{r})|_{x=L} . \tag{A1d}$$

Inserting the ansatz (7) and eliminating the coefficients a_{1jk} to d_{1jk} leads to a coupled system of linear equations,

$$\sum_m \Big[\Big\{ A^-_{nm}v_0^2 + A^+_{nm}u_0^2 + \Big(\frac{ik_n^+}{\sigma} - 2Zp_F\Big)\delta_{nm}\Big\}\alpha_{1jm} + \Big\{ A^-_{nm}v_0^2 + A^+_{nm}u_0^2 - \Big(\frac{ik_n^+}{\sigma} + 2Zp_F\Big)\delta_{nm}\Big\}e^{ik_m^+L}\beta_{1jm} - \big(A^-_{nm} + A^+_{nm}\big)u_0v_0e^{-ik_m^-L}\gamma_{1jm} - \big(A^-_{nm} + A^+_{nm}\big)u_0v_0\,\delta_{1jm}\Big] = 2ip_j^+u_0 , \tag{A2a}$$

$$\sum_m \Big[\Big\{ A^-_{nm}v_0^2 + A^+_{nm}u_0^2 - \Big(\frac{ik_n^+}{\sigma} + 2Zp_F\Big)\delta_{nm}\Big\}e^{ik_m^+L}\alpha_{1jm} + \Big\{ A^-_{nm}v_0^2 + A^+_{nm}u_0^2 + \Big(\frac{ik_n^+}{\sigma} - 2Zp_F\Big)\delta_{nm}\Big\}\beta_{1jm} - \big(A^-_{nm} + A^+_{nm}\big)u_0v_0e^{i\varphi}\gamma_{1jm} - \big(A^-_{nm} + A^+_{nm}\big)u_0v_0e^{-ik_m^-L+i\varphi}\,\delta_{1jm}\Big] = 0 , \tag{A2b}$$

$$\sum_m \Big[\Big\{ A^-_{nm}u_0^2 + A^+_{nm}v_0^2 - \Big(\frac{ik_n^-}{\sigma} - 2Zp_F\Big)\delta_{nm}\Big\}e^{-ik_m^-L}\gamma_{1jm} + \Big\{ A^-_{nm}u_0^2 + A^+_{nm}v_0^2 + \Big(\frac{ik_n^-}{\sigma} + 2Zp_F\Big)\delta_{nm}\Big\}\delta_{1jm} - \big(A^-_{nm} + A^+_{nm}\big)u_0v_0\,\alpha_{1jm} - \big(A^-_{nm} + A^+_{nm}\big)u_0v_0e^{ik_m^+L}\beta_{1jm}\Big] = -2ip_j^+v_0 , \tag{A2c}$$

$$\sum_m \Big[\Big\{ A^-_{nm}u_0^2 + A^+_{nm}v_0^2 + \Big(\frac{ik_n^-}{\sigma} + 2Zp_F\Big)\delta_{nm}\Big\}\gamma_{1jm} + \Big\{ A^-_{nm}v_0^2 + A^+_{nm}u_0^2 - \Big(\frac{ik_n^-}{\sigma} - 2Zp_F\Big)\delta_{nm}\Big\}e^{-ik_m^-L}\delta_{1jm} - \big(A^-_{nm} + A^+_{nm}\big)u_0v_0e^{ik_m^+L-i\varphi}\,\alpha_{1jm} - \big(A^-_{nm} + A^+_{nm}\big)u_0v_0e^{-i\varphi}\,\beta_{1jm}\Big] = 0 . \tag{A2d}$$

The coupling between subbands n and m is described by the factors

$$A^{\pm}_{nm} = (u_0^2 - v_0^2)^{-1}\sum_j \langle n|q_j\rangle\, ip_j^{\pm}\, \langle q_j|m\rangle . \tag{A3}$$

The Kronecker symbol δ_{nm} should not be confused with the coefficient δ_{1jm}. Solutions α_{1jm} to δ_{1jm} of Eqs. (A2) yield the coefficients

$$a_{1jk} = -(u_0^2 - v_0^2)^{-1}\sum_m \langle q_k|m\rangle\Big[\big(\alpha_{1jm} + \beta_{1jm}e^{ik_m^+L}\big)v_0 - \big(\gamma_{1jm}e^{-ik_m^-L} + \delta_{1jm}\big)u_0\Big] , \tag{A4}$$

from which we can calculate the current according to Eq. (11). It is impossible to solve the infinite system of equations (A2) exactly. However, a closer look at the factors $A^{\pm}_{nm}$ reveals that the off-diagonal ones ($n \neq m$) are orders of magnitude smaller than the diagonal ones ($n = m$). Therefore we neglect the off-diagonal factors and are left with four equations yielding the four coefficients α_{1jm} to δ_{1jm}, i.e., the equations for different subbands decouple. Equation (12) describes the resulting Josephson current.

To see the difference in order of magnitude between $A^{\pm}_{nm}$ for $n = m$ and $n \neq m$, we notice that at typical carrier densities ($n_s \sim 10^{12}$ cm^{-2}), only the lowest two or three subbands contribute propagating states.[16] The corresponding subband wave functions vary on the length scale $D \approx 5$ nm, so the matrix elements $\langle n|q_j\rangle$ vanish rapidly for $q_j \gtrsim 1/D$. The orthogonality of $|n\rangle$ and $|m\rangle$, $n \neq m$, implies that $A^{\pm}_{nm}$ is small unless $p_j^{\pm}$ varies appreciably with q_j over the range where the matrix elements are non-negligible (when the $p_j^{\pm}$ were independent of q_j, the off-diagonal $A^{\pm}_{nm}$ would vanish exactly). For all propagating states in the 2DEG, we have $k_y \leq k_{F,0} \ll p_F$. Only QP states of low energy, $E \sim \Delta_0$, are occupied, so $(2m_e/\hbar^2)\Omega \ll p_F^2$. Looking at Eq. (10a), we infer that $p_j^{\pm}$ is nearly equal to p_F in the whole range of q_j where $\langle n|q_j\rangle$ is non-negligible. A quantitative estimate can be obtained by expanding $p_j^{\pm}$ in a Taylor series for small q_j

and utilizing

$$\sum_j |q_j\rangle\, q_j^2\, \langle q_j| = -\frac{d^2}{dz^2}\,. \tag{A5}$$

This relation can be used in Eq. (A3) since the subband wave functions $\zeta_m(z)$ are negligibly small at $z = W$. The evaluation of $A_{nm}^{\pm}$ is then reduced to integrals over Airy functions, which can be performed exactly.[18] Thus we find that the ratio of off-diagonal to diagonal $A_{nm}^{\pm}$ is of order $(p_F D)^{-2} \approx 10^{-3}$. In summary, the point is that all relevant subband wave functions have an effective wavelength which is large compared to the Fermi wavelength of the superconductor. The shape of the confining potential in the 2DEG is less important.

[1] A. W. Kleinsasser and W. J. Gallagher, in *Superconducting Devices*, edited by S. T. Ruggiero and D. A. Rudman (Academic Press, San Diego, 1990).

[2] C. Nguyen, J. Werking, H. Kroemer, and E. L. Hu, Appl. Phys. Lett. **57**, 87 (1990).

[3] J. Nitta, T. Akazaki, H. Takayanagi, and K. Arai, Phys. Rev. B **46**, 14286 (1992).

[4] H. Takayanagi and T. Kawakami, Phys. Rev. Lett. **54**, 2449 (1985).

[5] K. Inoue and T. Kawakami, J. Appl. Phys. **65**, 1631 (1989).

[6] V. Z. Kresin, Phys. Rev. B **34**, 7587 (1986).

[7] Y. Tanaka and M. Tsukada, Solid State Commun. **61**, 445 (1987).

[8] Y. Tanaka and M. Tsukada, Solid State Commun. **65**, 287 (1988).

[9] G. Deutscher and P. G. de Gennes, in *Superconductivity*, edited by R. D. Parks (Marcel Dekker, New York, 1969).

[10] A. Furusaki and M. Tsukada, Solid State Commun. **78**, 299 (1991).

[11] A. Furusaki, H. Takayanagi, and M. Tsukada, Phys. Rev. B **45**, 10563 (1992). To compare our Eq. (12) to Eq. (5.3) of this paper, one must replace the continuous variable k_y by a discrete wave number, discard the subband energies E_m, and the width of the quantum point contact has to be held constant.

[12] P. G. de Gennes, *Superconductivity of Metals and Alloys* (Benjamin, New York, 1966).

[13] G. E. Blonder, M. Tinkham, and T. M. Klapwijk, Phys. Rev. B **25**, 4515 (1982).

[14] T. Ando, A. B. Fowler, and F. Stern, Rev. Mod. Phys. **54**, 437 (1982).

[15] Y. Tanaka and M. Tsukada, Phys. Rev. B **42**, 2066 (1990).

[16] A. Chrestin, Diplomarbeit, Universität Hamburg, 1993 (unpublished).

[17] U. Schüssler and R. Kümmel, Phys. Rev. B **47**, 2754 (1993).

[18] R. G. Gordon, J. Chem. Phys. **51**, 14 (1969).

[19] H. A. Antosiewicz, in *Handbook of Mathematical Functions*, edited by M. Abramowitz and I.A. Stegun (Dover Publications, New York, 1972).

[20] A. L. Gudkov, M. Y. Kupriyanov, and K. K. Likharev, Zh. Eksp. Teor. Fiz. **94**, 319 (1988) [Sov. Phys. JETP **68**, 1478 (1988)].

[21] P. G. de Gennes, Rev. Mod. Phys. **36**, 225 (1964).

[22] R. A. Morrow and K. R. Brownstein, Phys. Rev. B **30**, 678 (1984).